ELSEVIER

Polymer 41 (2000) 3797–3807

polymer

The ductile–brittle transition of irradiated isotactic polypropylene studied using simultaneous small angle X-ray scattering and tensile deformation

X.C. Zhang, M.F. Butler, R.E. Cameron*

Department of Materials Science and Metallurgy, University of Cambridge, New Museums Site, Pembroke Street, Cambridge, CB2 3QZ, UK

Received 4 November 1998; received in revised form 22 June 1999; accepted 30 July 1999

Abstract

This research concerns the micromechanical deformation mechanisms of irradiated and non-irradiated isotactic polypropylene (iPP), studied as a function of temperature above the glass transition. Several deformation mechanisms were identified and included lamellar separation, shear, stable and unstable fibrillated deformation and cavitation. The ductile–brittle transition rises dramatically with irradiation, while the glass transition shows only a small increase. This observation is explained by irradiation, through chain scission and cross-linking, having a dominant effect on large-scale plastic deformation, and a lesser effect on the deformation which relies on the amorphous phase alone.

Keywords: Ductile–brittle transition; Tensile deformation micromechanisms; Isotactic polypropylene

1. Introduction

Polypropylene is an important structural material. In some circumstances, for example during sterilisation for medical applications, it is subjected to significant doses of gamma irradiation, inducing significant change in mechanical properties. The response of the semi-crystalline structure to mechanical stress, before and after irradiation, is therefore of considerable interest. This research concerns the micromechanical deformation mechanisms of irradiated and non-irradiated isotactic polypropylene (iPP).

Isotactic polypropylene is a semi-crystalline polymer, which may crystallise into one of the three isomorphs, termed α, β and γ [1]. Conventional thermal processes result in spherulites with crystals of the monoclinic α isomorph [1]. All such spherulites possess radial lamellae, but under certain crystallisation conditions, tangential lamellae may also be present [2–7]. It is reported that most bulk crystallised samples contain spherulites of mixed character [3] in which some areas of the spherulite are richer in tangential lamellae than others [6]. A range of spherulite types will be present if the crystallisation temperature is not constant.

Polypropylene subjected to gamma irradiation undergoes cross-linking and scission [8,9]. In the presence of air, oxidation will enhance these effects [9]. Post irradiation ageing may occur as free radicals formed during irradiation react after the irradiation has ceased [9,10].

In another paper [11] we report studies on isotactic polypropylene which indicate that irradiation in air to 50 kGy causes the crystallinity to increase slightly and the glass transition temperature to rise by a few degrees. The changes to the dimensions of the lamellar architecture are small. It is widely reported however, that radiation does introduce major deterioration in mechanical properties of polypropylene as a consequence of chain scission and cross-linking [12–17].

Several modes of deformation above the glass transition have been identified in semi-crystalline polymers [18,19]. Initially, deformation occurs by strain in the interlamellar amorphous regions by a combination of inter-lamellar separation, stack rotation and inter-lamellar shear [20,21]. At yield, crystal shear may begin and the lamellar crystals begin to disintegrate [18–20]. “Fine chain slip” and “coarse chain slip” occurs which may result in a structure of semi-crystalline fibrils [18]. In polyethylene and polypropylene, a new fibril long spacing appears which differs from the spacing in the original spherulitic material [21]. An alternative model of melting and oriented recrystallisation in fibrillar morphology has also been proposed [22–24].

In tension, the plastic deformation occurring as crystals break up may be accompanied by voiding. This is easily initiated in the plane perpendicular to the load, as the polymer resists compression from Poisson contraction

* Corresponding author. Tel.: +44-1223-334-324; fax: +44-1223-334-567.

E-mail address: rec11@cam.ac.uk (R.E. Cameron).

0032-3861/00/$ - see front matter
PII: S0032-3861(99)00594-7

[25]. Friedrich [20] describes how individual blocks of crystals are pulled out of lamellae resulting in ellipsoidal defects between them. Fibrils are formed out of partly extended tie molecules and occasional blocks of folded crystal. The structure develops as the fibrils stretch, the chains within them aligning, and the voids coalesce laterally. The deformation zone then grows as more matrix material is drawn into it, and as the fibrils elongate. Eventually, the fibrils break giving a crack [25].

The fibrillar structures formed superficially resemble crazes seen in glassy amorphous polymers [26], but their mechanism of formation is different in semi-crystalline polymers above the glass transition [27]. In this paper, we will refer to "fibrillated shear" rather than "crazing" when considering deformation above the glass transition temperature [28].

The nature of the deformation is affected by the fine structure of the semi-crystalline morphology. If the crystals are thin, then less stress is required to induce them to shear and the yield stress is low using the dislocation model [29–31], alternatively the crystals are less stable and more easily melted in the melting–recrystallisation model [22–24]. A low tie chain density gives a greater transferral of load onto the crystallite and again favours a low yield stress [31]. The fibril strength, and hence the strength of the fibrillar deformation zones, is nearly proportional to the volume fraction of tie molecules [32] and the brittle fracture stress increases as this fraction rises [33].

In this paper we report experiments using simultaneous SAXS and tensile testing of bulk samples of polypropylene. The real time experiments allow the study of deformation without subsequent relaxation enabling the pre-yield deformation in particular to be followed accurately [34–37]. We explore the effects of deformation temperature and irradiation on the micromechanisms of deformation observed.

2. Materials and sample preparation

Isotactic polypropylene of average molecular weight, M_w, 250 000 was obtained from Sigma–Aldrich. The material was compression-moulded into plaques 1 mm thick and 160 mm wide with the following method. First the powder was heated to 190°C for 10 min, then the moulding pressure was increased to 3 MPa. The temperature was maintained at 190°C for a further 10 min although the pressure was allowed to fall. The mould and polymer were then plunged into a large bath filled with water maintained at 10°C.

Gamma irradiation was carried out by the Atomic Energy Authority using a ^{60}Co gamma ray source. The samples were sealed in glass tubes filled with either air or nitrogen and were irradiated up to doses of 50 kGy at a rate of 160 kGy/h at approximately 20°C. To minimise post irradiation effects, specimens were stored at −26°C (well below the glass transition of the polymer [38]) after completion of the irradiation.

Two types of tensile bar were prepared from the compression-moulded plaques. The first were standard dumbbell shaped tensile bars of gauge length 9 mm and width 3.8 mm. These samples were used for standard tensile deformation experiments. The second type were made by taking a 50 mm by 20 mm rectangular bar from the compression moulded plaques, and cutting out two semi-circular sections, with a radius of 7.5 mm, from the long sides. This left a minimum width of 5 mm at the centre of the specimen. These samples were used for simultaneous SAXS/deformation experiments. The design ensured that deformation and fracture always occurred at the centre of the sample where the X-ray beam was targeted. When the sample necks, the stress and strain distribution is constant throughout the neck, because it is formed from material pulled from the edges. The beam can always be situated so that it hits the neck (maximally deformed region), even though it will not pass through the centre of symmetry of the sample. When the sample is brittle, the extension is so low, and the beam size is so large on the sample, that the beam always passes through the cracked region. Obviously, because of the beam size, the X-ray data will always come from a material experiencing a range of strains. A full discussion of the limitations of this technique is given by Butler and Donald elsewhere [37].

3. Experimental

3.1. Tensile testing

Tensile tests on the standard tensile specimens irradiated in air and nitrogen to 0, 5, 15, 30 and 50 kGy were conducted at a cross-head speed of 10 mm/min on a Rheometric Scientific Miniature Materials Tester (Minimat) under PC control and equipped with a temperature controlled chamber. Deformation in the temperature range from −20 to 120°C was performed.

3.2. SAXS/tensile testing

Simultaneous SAXS/tensile testing experiments were performed on station 2.1 of the Synchrotron Radiation Source at the CLRC Daresbury Laboratory [39]. The experimental set up was similar to that reported elsewhere [34,35]. The Minimat was mounted in the path of the beam. SAXS patterns were recorded at intervals of 15 s on a gas-filled multi-wire area detector and the load-displacement curve was recorded simultaneously. Samples were mounted with a cross-head separation of 25 mm and deformed at a cross-head speed of 0.5 mm/min at temperatures between 20 and 120°C. Samples irradiated to 0 and 50 kGy, in air and nitrogen, were tested.

The shape of the non-standard tensile bars means that stress and strain could not be measured and a load displacement curve must therefore be used. (Although a rough comparison might be made by normalising at the yield

point, this would be misleading because the strains above and below it would not scale in the same way.) Furthermore, the strain rate could not be directly calculated from the cross-head speed as is the case for a standard tensile specimen. The strain rate in the central region will be larger than that which would be observed for a standard bar deformed at the same cross-head speed. This magnification will be particularly marked during necking.

The SAXS data were divided by the detector response obtained from uniform illumination by a ^{55}Fe source, normalised to the signal from an ionisation chamber placed behind the sample and a background subtracted. The scattering angle was calibrated in both the meridional and equatorial directions using wet rat tail collagen.

The long period in the meridional and equatorial directions was determined for each scattering pattern by taking radial slices and fitting the resulting intensity profiles with Gaussian peaks. The initial two points of data are less reliable since in this region the sample was not yet fully strained. No value was recorded if void scattering overlapped the lamellar peak. The Porod region of the void scattering overlapped with the lamellar scattering peak and a reliable separation of the two elements was not possible. Calculation of the scattering power was made impossible by the Poisson contraction of the sample and the fact that the exact strain was not known owing to the shape of the tensile specimen. Only qualitative analysis of void scattering was therefore attempted.

4. Results and discussion

4.1. Morphology

The morphology of samples prepared by the method used in this research has been reported elsewhere [11]. From wide angle X-ray scattering, the crystallinity of the samples was estimated as 53.2%. This rose very slightly to 55.6% after irradiation to a dose 50 kGy in air. The average long period remained largely unchanged by the irradiation. The fast cool resulted in small spherulites, measured by scanning electron microscopy (SEM) to be about 0.2–0.5 μm in radius [11]. This thermal history also means that it is likely that there is some degree of cross-hatching in the lamellar structure [6]. The glass transition temperature, as measured by DMTA at 3°C/min at a frequency of 1 Hz rose slightly from 10 to 15°C after 50 kGy irradiation in air. This change was attributed to a greater degree of constraint in the amorphous phase caused by cross-linking and the small amount of crystallisation presumably facilitated by chain scission.

4.2. Classes of deformation behaviour

Fig. 1 shows a map of brittle and ductile deformation as a function of the irradiation dose in air and the temperature of deformation, obtained from the standard tensile tests. Fracture was termed ductile and brittle on the basis of the failure

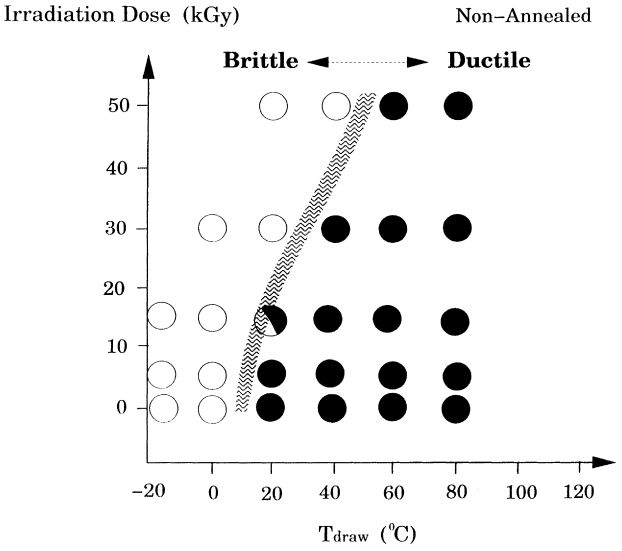

Fig. 1. Deformation map showing ductile and brittle behaviour as a function of irradiation dose and drawing temperature for a sample of iPP compression-moulded at 190°C and fast cooled to 10°C. Irradiation was performed at 20°C in air.

strain. Samples were termed ductile if they failed post yield, and brittle if they failed pre-yield or at yield. The ductile–brittle temperature rises as the irradiation dose increases.

The results from the simultaneous SAXS/tensile deformation studies showed four distinct classes of behaviour. Figs. 2–5 show typical load-displacement curves, 2D-SAXS patterns and meridional and equatorial long periods for each class. “Type L” behaviour is ductile and is typified by non-irradiated polypropylene at 80°C, shown in Fig. 2. “Type LF(U)” behaviour is brittle and typified by polypropylene irradiated to 50 kGy in air and deformed at 45°C is shown in Fig. 3. “Type LF(S)” behaviour is ductile and typified by polypropylene irradiated to 50 kGy in air and deformed at 80°C is shown in Fig. 4. The final type of deformation seen in the samples observed is “type LCF(S)”, seen in non-irradiated material deformed at 20°C (Fig. 5).

4.3. Type L: lamellar shear

Typical “type L” behaviour is shown in Fig. 2. Before yield, defined as the maximum in the load-extension curve, the meridional long period increases. This effect may be explained by extension of the amorphous layers leading to separation of the lamellae [40–45]. The equatorial long period decreases although the change is less marked than in the meridian. Simultaneous rotation and interlamellar shear between lamellae inclined to the loading direction may account for this effect [34,35]. The change in long period is relatively small because the amorphous layers are largely incompressible and since combined rotation and shear are required to change the long period. The intensity concentrates on the meridian as a result of the orientation of the lamellar normals towards the tensile axis.

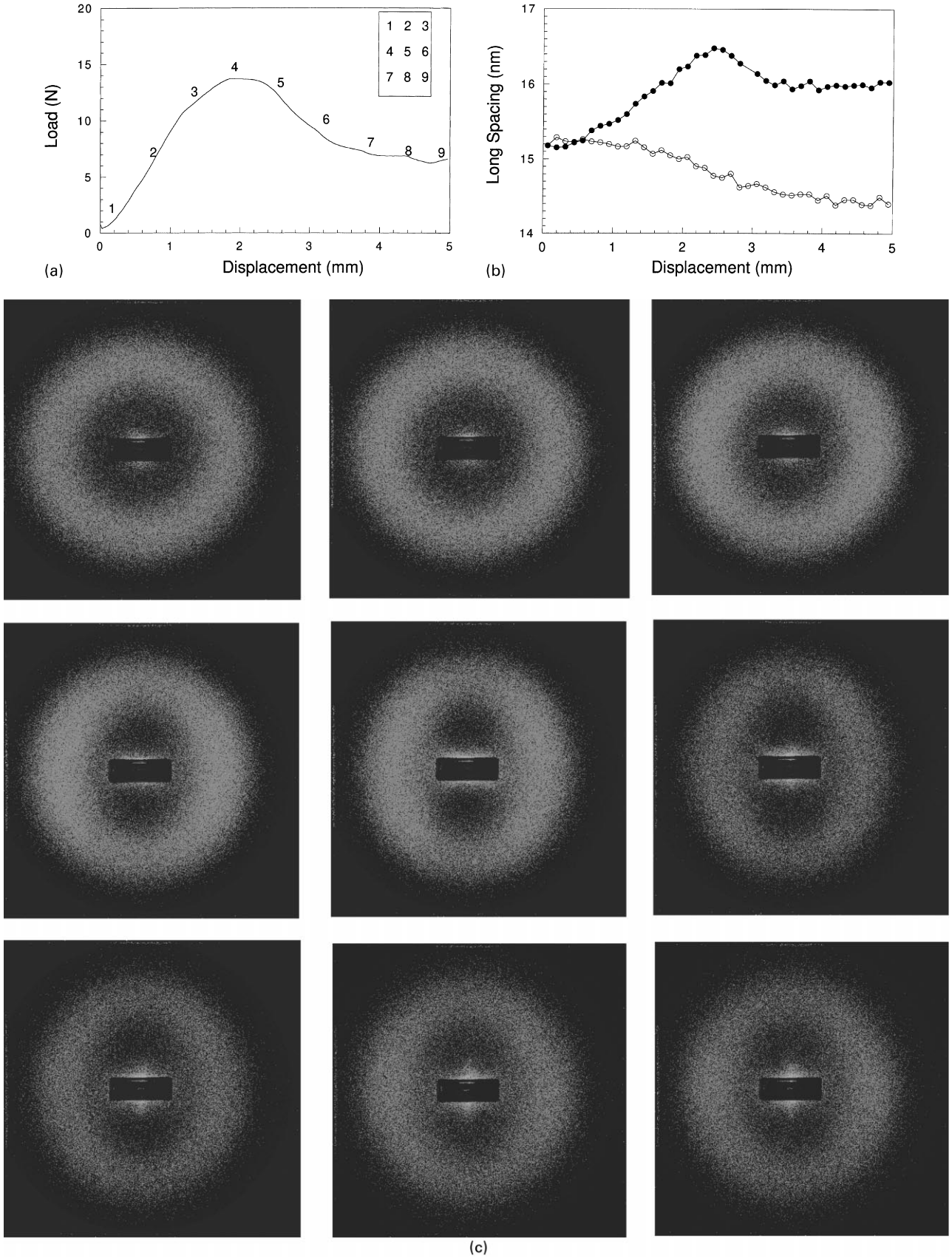

Fig. 2. The deformation behaviour of non-irradiated material, deformed at 80°C. The load-displacement curve is shown (a), with SAXS patterns corresponding to particular points on the curve (c). The evolution of the meridional (closed symbol) and equatorial (open symbol) long spacing with displacement are also shown (b). This behaviour is ductile and is typical of those termed “Type L” or “Lamellar Shear” in the text.

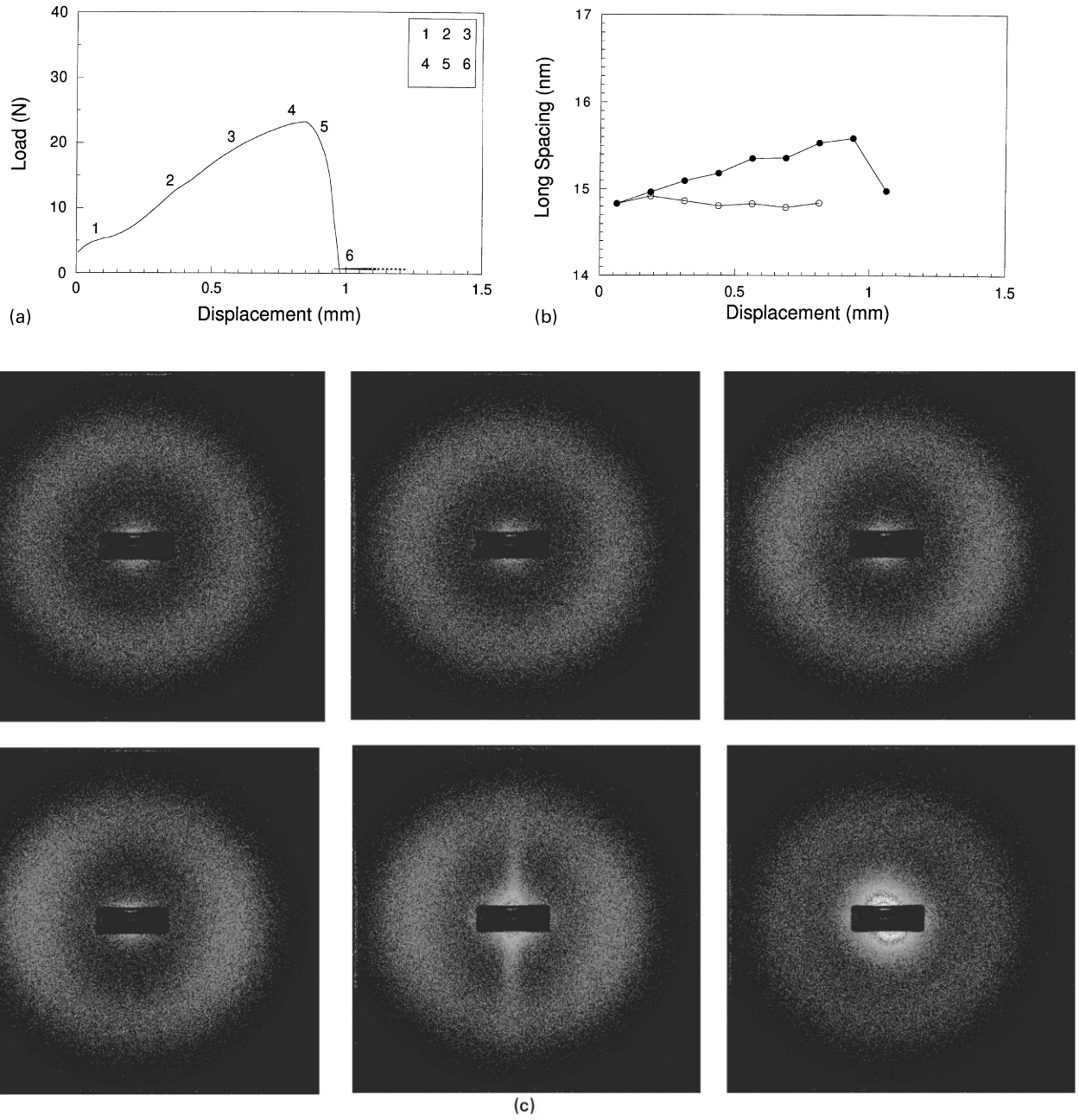

Fig. 3. The deformation behaviour of material irradiated in air to 50 kGy and deformed at 45°C. The load-displacement curve is shown (a), with SAXS patterns corresponding to particular points on the curve (c). The evolution of the meridional (closed symbols) and equatorial (open symbols) long spacing with displacement are also shown (b). This behaviour is brittle and is typical of those termed "Type LF(U)" or "Lamellar Shear and Unstable Fibrillated Shear" in the text.

Changes in the electron density differences between crystalline and amorphous material as the amorphous phase extends may also play a role in increasing the observed intensity.

At yield, the sample begins to neck and the load drops. It then reaches a relatively constant value as new material is drawn into the neck. This behaviour is correlated with the microstructural information. The meridional long period falls and reaches a plateau at about the same displacement, as the load becomes constant. The change in long spacing is likely to be due to the change from a lamellar to a microfibrillar morphology [21]. This transformation may be effected either by coarse chain slip, melting and oriented recrystallisation or both [18,21–24]. The equatorial long period falls in this regime. This may be interpreted as chain slip leading to shear within the crystals [34,37].

As the material draws, the observed scattering pattern stops changing, deformation is now occurring by drawing more material into the neck, in regions away from the X-ray beam. No void scattering is seen at any stage. Presumably

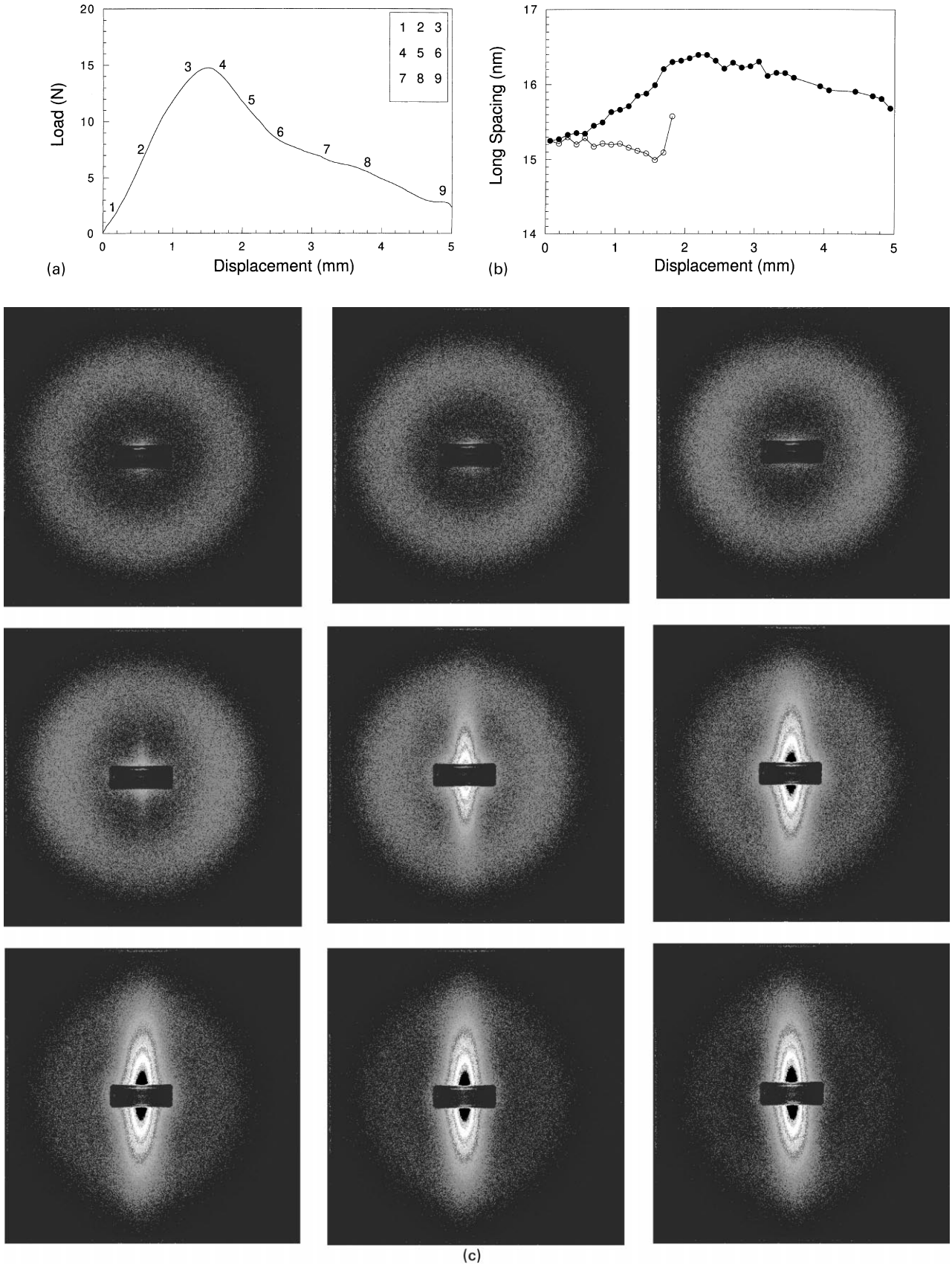

Fig. 4. The deformation behaviour of material irradiated in air to 50 kGy and deformed at 80°C. The load-displacement curve is shown (a), with SAXS patterns corresponding to particular points on the curve (c). The evolution of the meridional (closed symbols) and equatorial (open symbols) long spacing with displacement are also shown (b). This behaviour is ductile and is typical of those termed "Type LF(S)" or "Lamellar Shear and Stable Fibrillated Shear" in the text.

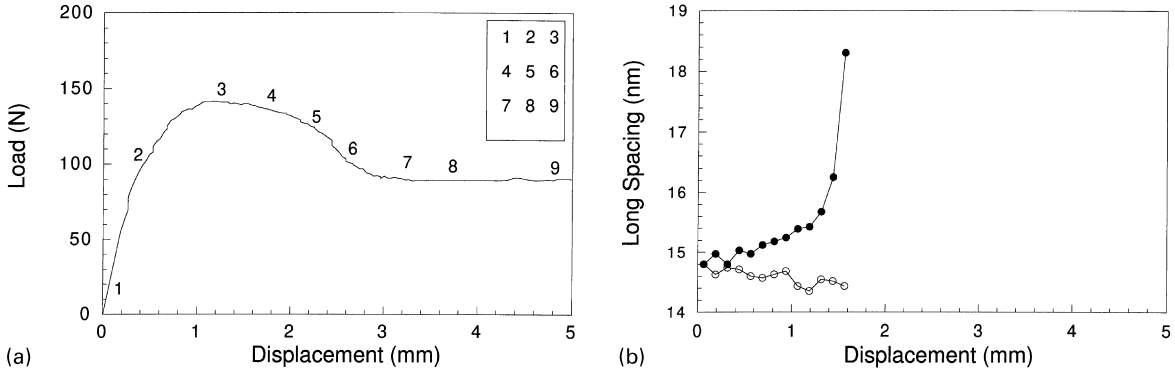

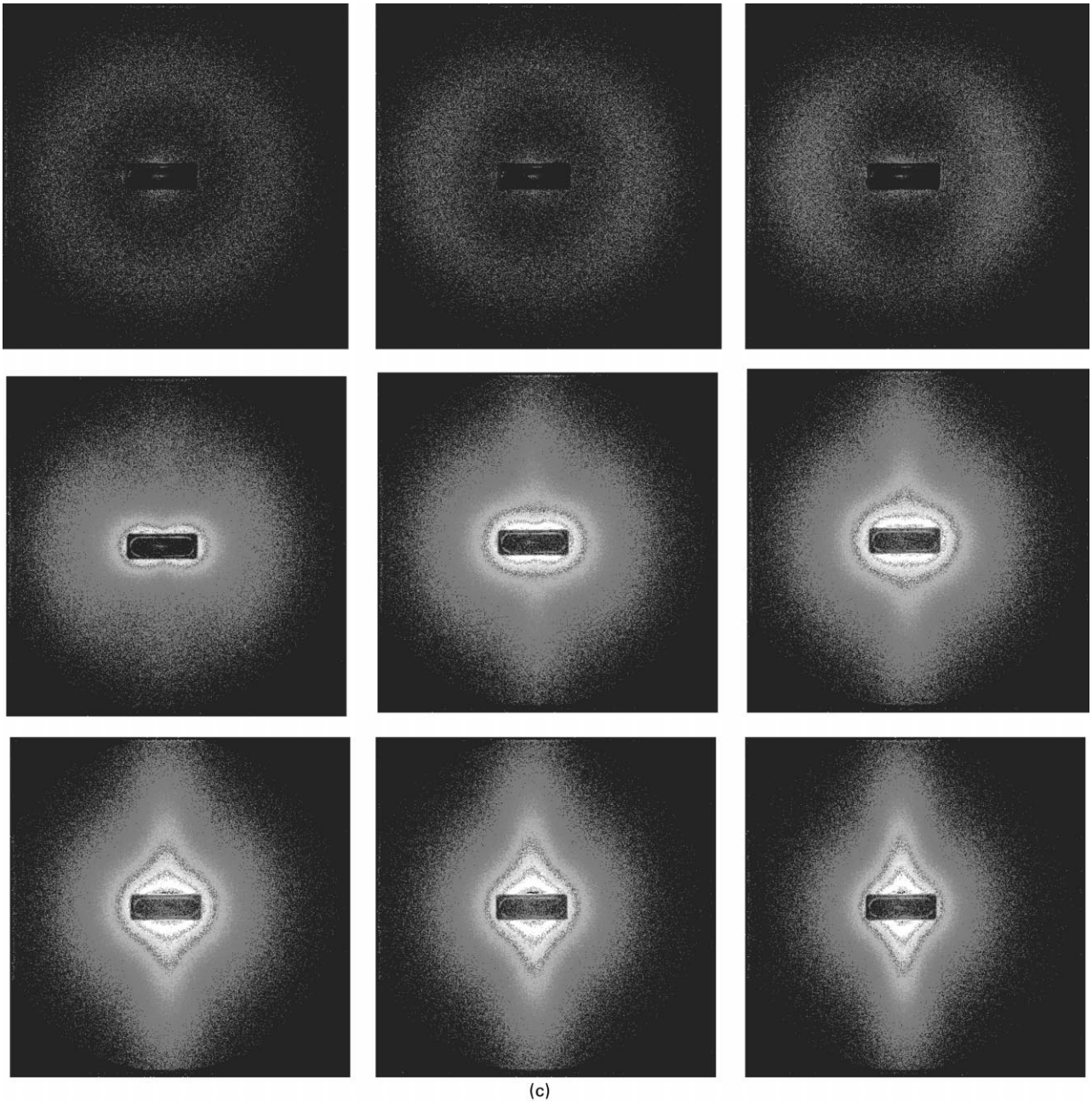

Fig. 5. The deformation behaviour of non-irradiated material, deformed at 20°C. The load-displacement curve is shown (a), with SAXS patterns corresponding to particular points on the curve. The evolution of the meridional (closed symbols) and equatorial (open symbols) long spacing with displacement are also shown (b). This behaviour is ductile and is termed “Type LCF(S)” or “Lamellar Shear, Cavitation and Stable Fibrillated Shear” in the text.

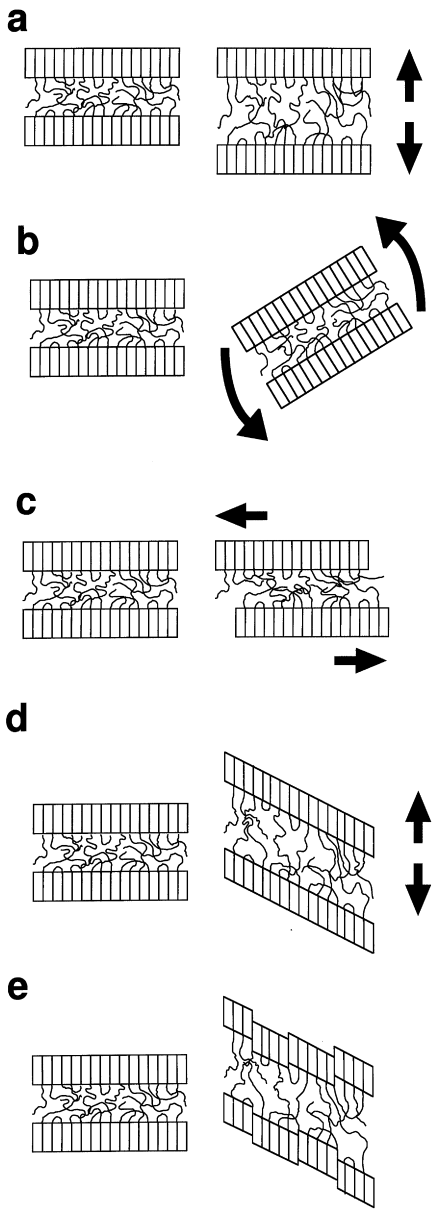

Fig. 6. Schematic diagram showing the variety of deformation mechanisms operative in a semi-crystalline polymer: (a) interlamellar separation, (b) lamellar stack rotation, (c) interlamellar shear, (d) intracrystalline shear ('fine chain slip'), (e) intracrystalline shear ('coarse chain slip'). In bulk samples, these mechanisms coexist.

deformation of the crystals is sufficiently easy for deformation of the whole structure to occur without the voiding which occurs in the types of behaviour described below. Fig. 6 schematically illustrates the microstructural changes during "type L" behaviour.

The above behaviour is similar to that seen in similar experiments on polyethylene [34–37]. This is noteworthy, since the polypropylene samples studied here are likely to have a cross-hatched texture (i.e. contain tangentially as well as radially oriented lamellae) and this might be expected to influence the micromechanisms of deformation observed. Tangential lamellae would be expected to hinder

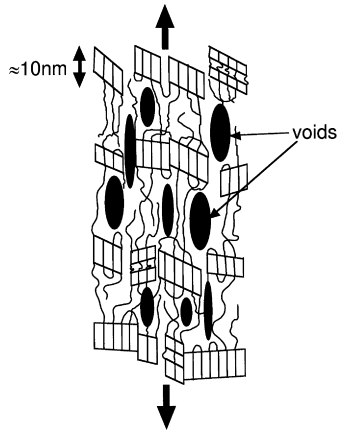

Fig. 7. Schematic diagram showing fibrillated shear in a semi-crystalline polymer.

rotation of the lamellae in the initial regime of deformation. Way and Atkinson [46] and Peterlin [22] studied differences in the microstructure of bulk isotactic polypropylene and polyethylene deformed at room temperature then sectioned to allow microscopy. In polyethylene, drawing occurred along diameters perpendicular to the stress, since the weakest links were along the lamellae. In isotactic polypropylene, yield was first seen along the faces of tangential lamellae lying across the stress axis rather than radial lamellae. The deformation zone propagated perpendicular to the stress, following lamellar faces. Isotactic polypropylene would be expected to deform more isotropically than polyethylene because the tangential lamellae give it greater strength in the tangential direction, while weakening the radial direction. The data presented here suggests that the effect in our samples, if it exists, is not that great.

4.4. Type LF(U): lamellar shear and unstable fibrillated shear

"Type LF(U)" behaviour is shown in Fig. 3. As for "type L" shear, before the yield point, the meridional long period rises and the intensity concentrates on the meridian, indicating the operation of the inter-lamellar separation mechanism and lamellar rotation. Over the small displacements observed, there is little change in the equatorial long spacing. However, unlike "type L" behaviour, at the peak load an equatorial streak appears. We interpret this as localised "fibrillated shear" (F), in which the crystal break up is accompanied by the creation of long, thin voids or volumes of low density polymer oriented along the direction of force [20] (Fig. 7). In LF(U) deformation, the fibrils are unable to support the load and the material rapidly fails.

4.5. Type LF(S): lamellar shear and stable fibrillated shear

"Type LF(S)" behaviour is shown in Fig. 4. This begins in the same way as "type LF(U)" shear with lamellar shear (L) and fibrillated shear (F) at the yield point. However, in this

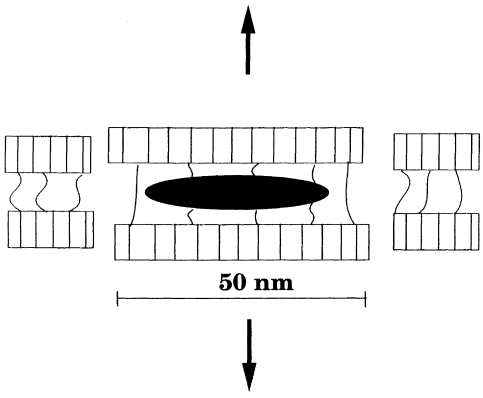

Fig. 8. Schematic diagram showing cavitation in a semi-crystalline polymer.

case the fibrils are strong enough to support the applied load. The material draws as fresh material is drawn into the neck. The void scattering becomes more intense as the material draws and the fibrillated shear becomes less localised.

4.6. Type LCF(S): lamellar shear, cavitation and stable fibrillated shear

The final type of deformation seen in the samples observed is "type LCF(S)" (Fig. 5). The pre-yield deformation is similar to those in the other samples. At the maximum stress, a new type of SAXS pattern appears at low angles consisting of two intense round lobes centred on the meridian making a peanut shell shape. This pattern corresponds to the signature from inhomogeneities which are large and elongated with the long axis oriented roughly perpendicular to the applied load. We interpret these entities as voids, or cavities, between some lamellae, and term this regime of deformation "cavitation", (C), (Fig. 8). Cavitation is most likely to occur between lamellae whose normals are parallel to the applied force and may also occur between spherulites. The scattering occurs at much lower angles than that from the lamellar repeat; therefore voiding does not occur between every crystal. The voids appear (during tensile deformation) before any large scale break up of the crystals and their formation is a necessary precursor [18] to intra-lamellar shear when the chains in the amorphous phase are constrained or crystal shear is difficult because of low temperatures or large crystal thickness.

As deformation develops the material necks and a lemon shaped scattering pattern appears. Two possible explanations may account for this observation. Firstly, the scattering may be a combination of scattering from cavitation and scattering from the voids formed during fibrillated shear, formed by two different mechanisms. This dual mechanism is possible since the lamellae vary in orientation throughout the spherulite, resulting in the operation of different local deformation mechanisms [47,48]. It is also possible that cavitation causes stress concentration on the remaining connections between crystals and fibrillated shear results. Secondly, a single mechanism may be in operation in which the initial cavities are elongated to form the voids normally associated with fibrillated shear and the scattering pattern results from the range of void shapes and sizes present at any one time [36].

4.7. Annealing and drawing

At 120°C, the samples starts to re-crystallise through annealing effects, indicating that at least some of the crystallisation of the sample occurred below this temperature (and hence that at least a partial cross-hatched structure is likely to be present [1,6]. The behaviour in these samples was complex since the two distinct processes of annealing and deformation were occurring simultaneously. These samples will not be considered further in this paper.

4.8. Deformation in non-irradiated material

Since the spherulites were small (about 0.25–0.5 μm in radius), it is likely that yield occurred within the bulk of the spherulites in all cases. The critical spherulite radius for boundary yield in some samples of isotactic polypropylene was found to be much larger (about 80 μm in some samples [49]). However, boundary yield is more likely in thin films in any case because of the plane stress-state they experience and the fact that the films may be initially thinner at the boundaries anyway.

Fig. 9 shows a map of the deformation mechanism as a function of irradiation dose and conditions and the temperature of deformation. Areas in which the behaviour is ductile are shaded. The glass transition temperatures (as measured by DMTA at 3°C/min and 1 Hz [11]) are also marked. The non-irradiated material is above its glass transition temperature and ductile at all temperatures under the testing conditions imposed. At 20°C, the material is only slightly above its glass transition temperature and below the reported α relaxation [38]. Crystal shear is difficult under these conditions, so initially there is not enough stress to enable the crystals to shear. The material responds with perpendicular cavitation, perhaps until there is sufficient stress concentration on the crystals for fibrillated shear to begin. The fibrillated shear is stable and the LCF(S) mechanism is observed.

At higher temperatures α relaxation, of stepwise chain motion through the crystal structure, becomes activated. Owing to thermal expansion the crystal unit cell will also expand, reducing the van der Waals bond strength between chains in the crystal. Both these factors will make crystal shear much easier. The whole structure can deform now without voiding and "type L" behaviour is seen.

4.9. Deformation in irradiated material

Fig. 1 shows that in non-irradiated material, the ductile–brittle transition temperature, under the particular testing conditions utilised, corresponds quite closely to the glass

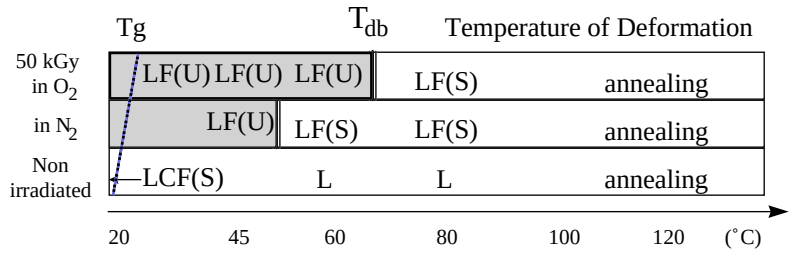

Fig. 9. A mechanism map showing the micromechanisms of deformation for polypropylene samples as a function of dose, irradiation atmosphere and temperature of deformation. Brittle deformation is indicated by shaded regions. The approximate glass transition, as measured using DMTA [11], is also indicated.

transition temperature. However, this is not the case for the irradiated material, where the glass transition temperature remains largely unchanged but the ductile–brittle transition temperature increases significantly. The key to these differences must lie with the changes induced by irradiation and their influence on the micromechanical deformation mechanisms.

The irradiated materials all deformed by lamellar shear followed by fibrillated shear. Below the ductile–brittle transition, the fibrillated shear was unstable. Above it, the fibrils were able to support the load and stable fibrillated shear was observed.

Irradiation is known to cause both chain scission and cross-linking in polypropylene [8]. Chain scission is particularly connected with oxidation [9], and hence the sample irradiated in air will have the lower molecular weight. Since the size of the crystals and the amorphous layers are largely unchanged by irradiation [11], the effects seen are unlikely to be related to these morphological features. Both chain scission and cross-linking, however, are likely to contribute to the raised ductile–brittle transition temperature and the changed micromechanical modes of deformation seen.

Chain scission will result in fewer tie chains between the crystals. This means that there will be greater local stress concentration on crystals in the irradiated material. The result is that crystal shear occurs at a lower overall stress and the shear operates without requiring cavitation as a stress concentrator, even at 20°C. The lower molecular weight makes the fibrils weaker by reducing their disentanglement resistance and hence brittle failure is seen at higher temperatures than in the non-irradiated material. The greater degree of oxidation and hence chain scission in the material irradiated in air means that this effect is greater and the ductile–brittle transition is raised still higher.

Cross-links caused by irradiation make propagation of the deformation zone more difficult by reducing chain mobility and inhibiting the stepwise motion of chains through the crystal. Therefore, it is harder for the material to respond to the imposed deformation though propagation of the neck and favours brittle failure. This reduction in mobility also pushes the ductile–brittle temperature to higher values.

At high temperatures ductile deformation is seen, through the LF(S) mechanism. The cross-links and chain scission effects described still favour fibrillation rather than simple lamellar shear (L) seen in the non-irradiated material. However, in this case crystal shear is favoured and the obstacles to deformation created by cross-links may be circumvented. The resultant fibrillar deformation zone is stable because the material can still flow.

The initial deformation in the pre-yield regime is little affected by irradiation. This observation is consistent with the largely unchanged glass transition temperature: the mobility of the amorphous layers is little affected and hence their response to load is similar. It is only when large-scale plastic deformation occurs that the changes in chain chemistry become important.

5. Conclusions

The micromechanisms of deformation of polypropylene and irradiated polypropylene have been explored using simultaneous SAXS/tensile deformation. Four types of deformation were observed in the system described. The mechanism–temperature relationships change with irradiation dose and environment and can be related to chain scission and cross-linking. Irradiation has a dominant effect on large-scale plastic deformation, and a lesser effect on the deformation, which relies on the amorphous phase alone.

Acknowledgements

The authors are grateful to British Nuclear Fuels Ltd., who funded this research. The SAXS data was obtained on station 2.1 of the CLRC Daresbury Laboratory with the assistance of Sue Slawson. Software from the CCP13 suite was employed in the analysis.

References

[1] Varga J. In: Karger Kocsis J, editor. Polypropylene: structure, blends and composites. London: Chapman and Hall, 1995.
[2] Padden Jr FJ, Keith HD. J Appl Phys 1973;44:1217.
[3] Norton DR, Keller A. Polymer 1985;26:705.
[4] Lotz B, Wittman JC. J Polym Sci, Polym Phys Ed 1986;24:1541.
[5] Olley RH, Bassett DC. Polymer 1989;30:399.

[6] Padden Jr. FJ, Keith HD. J Appl Phys 1959;30:1479.
[7] Idrissi BOB, Chabert B, Guillet J. Macromol Chem 1985;186:881.
[8] Nishimoto S, Kagiya T. Handbook of polymer degradation. In: Hamid SH, Amin MB, Maadhah AG, editors. Radiation degradation of polypropylene, New York: Marcel Dekker, 1992 chap. 1.
[9] Carlsson DJ, Chmela S. Mechanisms of polymer degradation and stabilisation. In: Scott G, editor. Polymers and high-energy irradiation: degradation and stabililisation. London: Elsevier, 1990 chap. 4.
[10] Carlsson DJ, Dobbin CJB, Jensen JPT, Wiles DM. Polymer stabilisation and degradation. ACS Symposium Series 1985;280:25.
[11] Zhang XC, Cameron RE. J Appl Polym Sci 1999;74:2234.
[12] Kagiya T, Nishimoto S, Watanabe Y, Kato M. Polym Degrad Stab 1985;12:261.
[13] Nishimoto S, Kitamura K, Watanabe Y, Kagiya T. Radiat Phys Chem 1991;37:71.
[14] Rolando RJJ. Plastic Film Sheeting 1993;9:326.
[15] Martakis N, Niaonakis M, Pissimissis D. J Appl Polym Sci 1994;51:313.
[16] Nishimoto S, Kagiya K, Watanabe Y, Kato M. Polym Degrad Stab 1986;14:199.
[17] Kholyou F, Katbab AA. Radiat Phys Chem 1993;42:219.
[18] Bowden PB, Young RJ. J Mater Sci 1974;9:2034.
[19] Lin L, Argon AS. J Mater Sci 1994;29:294.
[20] Friedrich K. Adv Polym Sci 1983;52/53:225.
[21] Peterlin A. J Mater Sci 1971;6:490.
[22] Juska T, Harrison IR. Polym Engng Sci 1982;22:766.
[23] Gent AN, Madan SJ. J Polym Sci, Polym Phys Ed 1989;27:1529.
[24] Meinel G, Peterlin A. J Polym Sci, Polym Phys Ed 1971;9:1967.
[25] Sugimoto M, Ishikawa M, Hatada K. Polymer 1995;36:3675.
[26] Kramer EJ. Adv Polym Sci 1983;52:1.
[27] Plummer CJG, Kausch HH. Polym Engng Sci 1994;34:318.
[28] More AP, Donald AM. Polymer 1992;33:4081.
[29] Schultz JM. Polym Engng Sci 1984;24:770.
[30] O'Kane WJ, Young RJ. J Mater Sci Lett 1995;14:433.
[31] O'Kane WJ, Young RJ, Ryan AJ. J Macromol Sci-Phys B 1995;34:427.
[32] Ishikawa M, Ushui K, Kondo Y, Hatada K, Gima S. Polymer 1996;37:5375.
[33] Brown N, Ward IM. J Mater Sci 1983;18:1405.
[34] Butler MF, Donald AM, Bras W, Mant GR, Derbyshire GE, Ryan AJ. Macromolecules 1995;28:6383.
[35] Butler MF, Donald AM, Ryan AJ. Polymer 1997;38:5521.
[36] Butler MF, Donald AM, Ryan AJ. Polymer 1998;39:39.
[37] Butler MF, Donald AM. Macromolecules 1998;31:6234.
[38] McCrum NG, Read BE, Williams G. Anelastic and dielectric effects in polymeric solids. New York: Dover, 1991.
[39] Towns-Andrews E, Berry A, Bordas J, Mant GR, Murray PK, Roberts K, Sumner I, Worgan JS, Lewis R. Rev Sci Instrum 1989;60:2346.
[40] Kaufman WE, Schultz JM. J Mater Sci 1973;8:41.
[41] Pope DP, Keller A. J Polym Sci, Polym Phys Ed 1975;13:533.
[42] Peterlin A, Meinel G. Makromol Chem 1971;142:227.
[43] Beresford DR, Bevan H. Polymer 1964;5:247.
[44] Slutsker AI, Sanphirova TP, Yastrebinskii AA, Kuksenko VC. J Polym Sci C 1967;16:4093.
[45] Ishikawa K, Miyasaka K, Maeda K, Yamada MJ. J Polym Sci, A2 1969;7:1259.
[46] Way JL, Atkinson JR. J Mater Sci 1971;6:102.
[47] Allan P, Bevis M. Philos Mag 1977;35:405.
[48] Allan P, Bevis M. Philos Mag 1980;41:555.
[49] Way JL, Atkinson JR, Nutting JJ. Mater Sci 1974;9:293.